Electronic Supplementary Material (ESI) for Sustainable Energy & Fuels.

Supporting Information

An Electrolyte-Affinity Hybrid Membrane with the Supporting of Polymer and Modification of Amphiphilic Block Copolymer for Superhigh-Flexible and High-Performance Supercapacitor

Xiaoning Zhao, Yunlong Yang, Jiayu Wu, Yongtao Tan, Ying Liu, Long Kang, Fen Ran*

State Key Laboratory of Advanced Processing and Recycling of Non-ferrous Metals,
Lanzhou University of Technology, Lanzhou 730050, P. R. China
*Corresponding authors: Fen Ran (ranfen@163.com; or ranfen@lut.cn)

2. Experimental

2.1. Chemicals

Polyether sulfone (PES, Ultrason E6020P) was obtained from *BASF*, Germany. Activated carbon was purchased from *Shenyang Kejing Auto-instrument Co. Ltd.* Vinylcyanide (AN) and acrylic acid (AA) from *Sinopharm Chemical Reagent Co. Ltd.* was further purified by distillation prior to use. $NiCl_2 \cdot 6H_2O$ was purchased from *Tianjin Beichen Founder Reagent Factory* and $NH_3 \cdot H_2O$ was obtained from *Tianjin BASF Chemical Co., Ltd*. All the other chemicals (analytical grade) were obtained from *Sinopharm Chemical Reagents Co. Ltd*, China, and used without further purification. Azo-bis-isobutryonitrile (AIBN) was purchased from Tianjin Tianhe Chemical Reagent Factory (Tianjin, China) and used as the initiator. RAFT agent was synthesized according to the literature [S1].

2.2. Synthesis of Nickel Hydroxide ($Ni(OH)_2$)

$Ni(OH)_2$ materials were prepared by a facile-improved precipitation method. In a typical procedure, 40 g of $NiCl_2 \cdot 6H_2O$ was dissolved in 141 mL deionized water in a glass beaker with magnetic stirring at room temperature. Then the $NiCl_2 \cdot 6H_2O$ solution was slowly adjusted to pH=9 by dropwise addition of 5 wt % $NH_3 \cdot H_2O$ at a temperature of 20 °C, controlling the addition time to more than 2 h. The resulting suspension was stirred at this temperature for an additional 3 h. Finally the solid was filtered and washed with a copious amount of distilled water, and dried at 60 °C for 6 h.

2.3. Synthesis of PAA-b-PAN-b-PAA

The general procedure for synthesis of polyacrylic acid (PAA) was as follows. AA, RAFT agent, AIBN and DMF were added into a tube. After bubbling for 30 min with nitrogen, the reaction mixture was allowed to warm under a nitrogen atmosphere to 75 °C, and the polymerization lasted for 4 h. After precipitating in ethyl ether, the product was dried under vacuum at 60 °C overnight.

The synthesis of *PAA-b-PAN-b-PAA* was carried out in a sealed tube, and shown as follows: acrylonitrile (AN), the macro-RAFT agent (PAA), AIBN and DMF were added to a tube, and stirred for 10 min. After bubbling with nitrogen for 30 min the reaction mixture was allowed to warm to 75 °C under a nitrogen atmosphere and polymerization was carried out for 12 h. After precipitation in ethyl ether the product was dried under vacuum at 60 °C overnight.

2.4. Preparation of Ultrathin Porous Membranes

The membranes were prepared by a phase-separation technique. In a typical synthesis, $Ni(OH)_2$ (1.7 g) mixed with acetylene black (0.15 g) and conducting graphite (0.15 g) were firstly dispersed in dimethylacetamide (DMAC) under magnetic stirring and ultrasonication to obtain a homogeneous turbid solution. Then, PES (0.45 g) and *PAA-b-PAN-b-PAA* (0.05 g) were dissolved in the solution and stirred for 24 h. The casting solutions were prepared as membranes by spin coating at 20 °C, which was immediately immersed in a coagulation bath of deionized water at 20 °C. Then, the ultrathin hybrid polymer-nickel hydroxide membranes were transferred to a water bath for 24 h to remove the residual solvent. Finally, the flexible membranes were dried in vacuum oven at 60 °C for 24 h named as FME-$Ni(OH)_2$. The FMEs without containing conductive agent (acetylene black and conducting graphite) or the block copolymer *PAA-b-PAN-b-PAA* were fabricated in the similar way, and named as FME-NC, and FME-NP, respectively. The hybrid polymer-carbon membrane was also prepared in the same conditions as FME-AC.

2.5 Materials Characterization

The microstructures and morphologies were characterized by field emission scanning electron microscope (SEM, JSM-6701F, JEOL, Japan) and transmission electron microscope (TEM, JEM-2010, JEOL, Japan). The photographs of were taken using a camera (PowerShot S100V, Canon, Japan). The crystal structure was analyzed by X-ray diffraction (XRD Bruker, D8 Advance, Germany). The surface area was calculated using the Brunauer-Emmett-Teller (BET) equation. Pore size distribution was calculated by the Barrett-Joyner-Halenda (BJH) method using the adsorption branch of the isotherm. The surface chemical compositions of the samples were analyzed by X-ray photoelectron spectroscope (XPS, physical Electronics UK).

2.6 Electrode Preparation

For the preparation of FME-$Ni(OH)_2$, FME-NP, FME-NC and FME-AC electrodes, a thin membrane of about 1×1 cm^2 was cut down from the membrane, and pressed between two foam nickels (Chang Sha Lyrun New Material Co. Ltd., 90 PPI, 2 mm) of 1.5 × 2 cm in size (the nickel foam functions as the current collector) at 10 MPa. The capacitance values were calculated based on the mass of $Ni(OH)_2$ and AC in the membranes, respecitvely. And the mass of FME-$Ni(OH)_2$, FME-NP, FME-NC and FME-AC electrodes were 2.5, 2.6, 3.7 and 8.6 mg, respectively. For comparison, the $Ni(OH)_2$ electrode was prepared by the traditional method according to the method reported in the literature. $Ni(OH)_2$ powder, acetylene black and conducting graphite at a mass ratio of 80: 7.5: 7.5 (wt %) was added in an agate mortar until a homogeneous black powder obtained. To this mixture, polytetrafluoroethylene (5 wt %) was added with a few drops of ethanol. The resulting paste was pressed at 10 MPa to nickel foam that served as a current collector then dried at 80 °C for 12 h. Each $Ni(OH)_2$ electrode contained 4 mg of the electroactive material and had a geometric surface area of 1 cm^2.

2.7 Electrochemical Characterization

All electrochemical measurements were conducted in a classical three-electrode glass cell setup at room temperature. The synthesized sample, platinum foil electrode (1.5 × 1.5 cm) and a saturated calomel electrode (SCE) served as working electrode, counter electrode and reference electrode, respectively. The performance of electrochemical properties was tested using cyclic voltammetry (CV), galvonostatic charge-discharge (GCD) and electrochemical impedance spectroscopy (EIS) in a CHI660E (Shanghai, China) electrochemical workstation. The cycle stability test was carried out on a land cell tester.

The electrochemical measurements of the asymmetric supercapacitor were carried out in a two-electrode, where the FME-$Ni(OH)_2$ and FME-AC were used as positive electrode and negative electrode, respectively. The mass ratio of the positive and negative electrodes (FME-$Ni(OH)_2$: FME-AC) was estimated to be 1:3 from the specific capacitor and potential window obtained from their galvanostatic charge-discharge curves. All of the above electrochemical measurements were performed in 6 M KOH aqueous solutions electrolytes.

2.8 The preparation of polymer gel electrolyte

The polymer gel electrolyte was prepared according to the method reported in literature [S2]. 2 g polyvinyl alcohol (PVA) was dissolved in 20 ml distilled water under continuous heating at 85 °C and stirring until the solution turned clear. Then, 4.2 g lithium chloride (LiCl) was slowly added with magnetic stirring and the solution was stirred for additional one hour. After cooling to room temperature, the PVA-LiCl gel electrolyte was obtained.

Calculations: The specific capacitance of electrode can be calculated from the discharge curves at different current densities by the equation:

$$C = I \times t / (\Delta V \times m) \qquad C_m = I \times t / m \qquad (1)$$

Where C (F/g), C_m (C/g) is the specific capacitance, I (A) is discharge current, t (s) is the discharge time, ΔV (V) is the potential drop during discharge process and m (g) is the mass of active materials.

The energy and power density of device are calculated from the discharge curves at different current densities using the following equations:

$$E=C \times V^2/(2 \times 3.6) \quad (2)$$

$$P= E \times 3600/(\Delta t) \quad (3)$$

Where E (Wh/kg) is the energy density of device, C (F/g) is the specific capacitance, V (V) is the potential drop during discharge process, P (W/kg) is the power density of device, and Δt (s) is the discharge time.

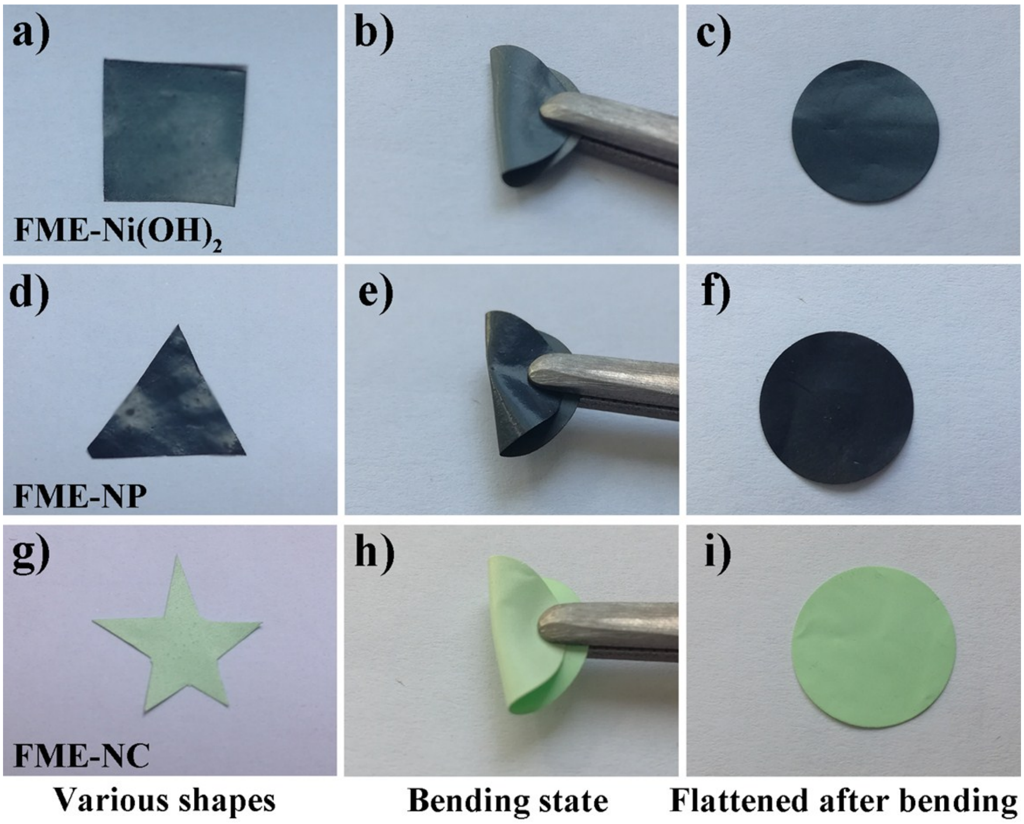

Figure S1 Digital photographs of the FMEs with excellent flexibility

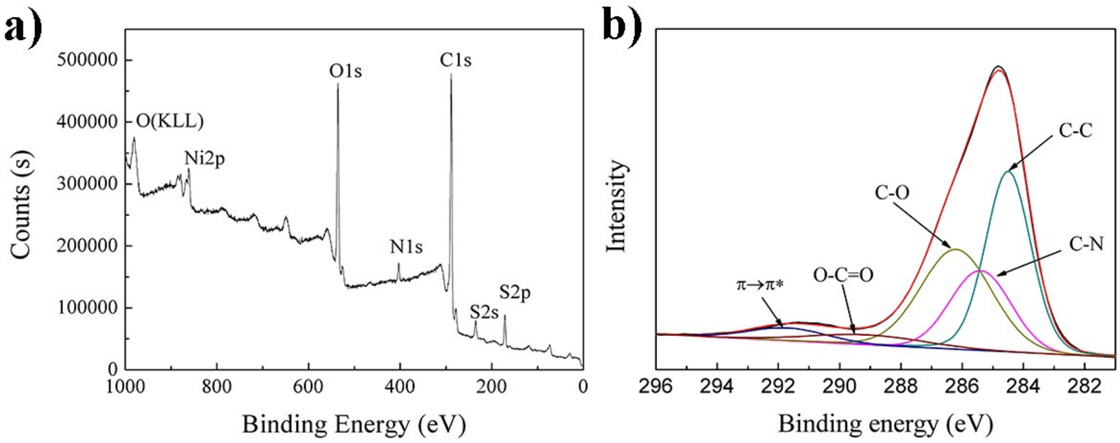

Figure S2 XPS spectrum (a) and C 1s XPS spectra (b) for the FME-$Ni(OH)_2$

The enrichment of the block copolymer PAA-*b*-PAN-*b*-PAA on the membrane surface can be confirmed by X-ray photoelectron spectroscope (XPS) analysis. The strong O 1s signal at the binding energy (BE) of 535 eV and N 1s signal at the BE of 403 eV in the wide scan spectrum (**Figure S2 a**) indicate the surface of FME-$Ni(OH)_2$ membrane was covered with PAA-*b*-PAN-*b*-PAA chains, and the Ni 2p signal at the BE of 859 eV suggest the existence of $Ni(OH)_2$. The C 1s core-level spectrum of the FME membrane surface was recorded and analyzed (**Figure S2 b**). It is curve-fitted into five peak components at 284.5, 285.4, 286.2, 289.7 and 291.9 eV, respectively attributable to the C-C, C-N, C-O, O-C=O and π→π* species [S3]. These results confirmed the existence of PAA and PAN blocks on the surface of FME-$Ni(OH)_2$. The appearing of π→π* peak can be attributed to the introduction of conductive additive (acetylene black and conducting graphite). All these results indicate that a porous, well electrical conductivity and electrolyte-affinity flexible membrane electrode material is fabricated successfully.

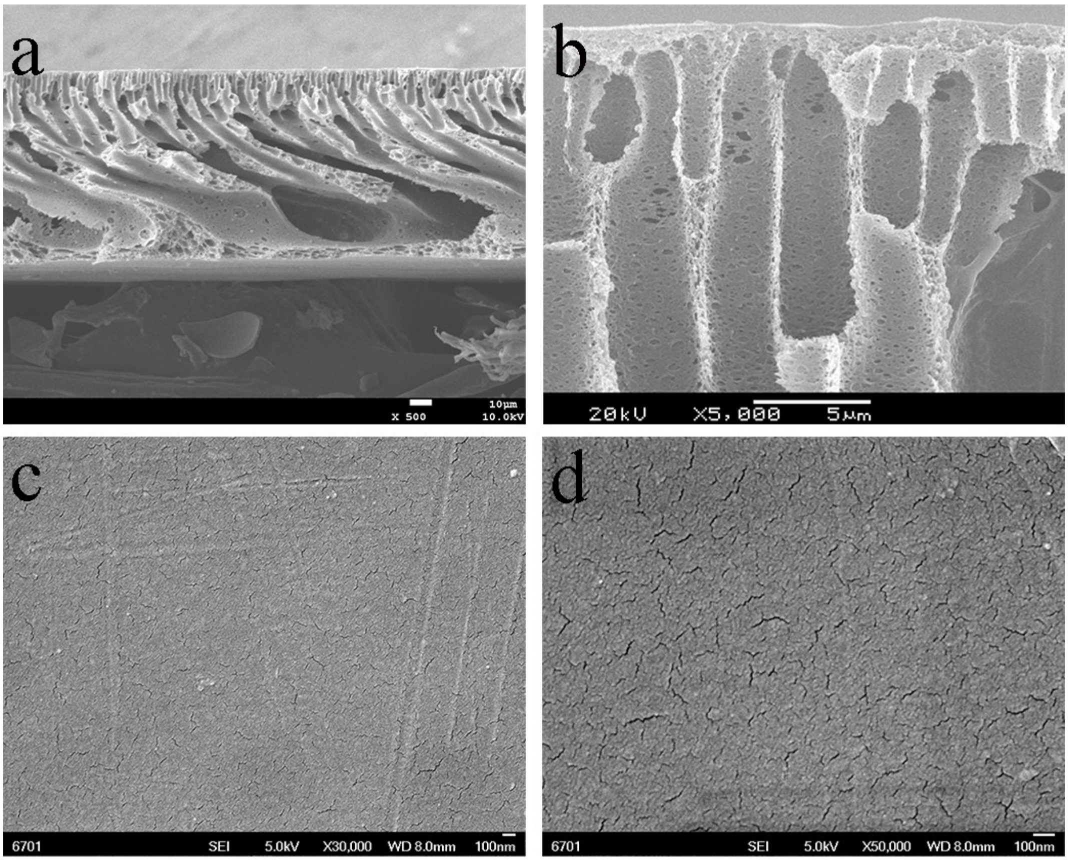

Figure S3 SEM images of PES membrane: a and b) the cross-sectional views; and c and d) the surface views

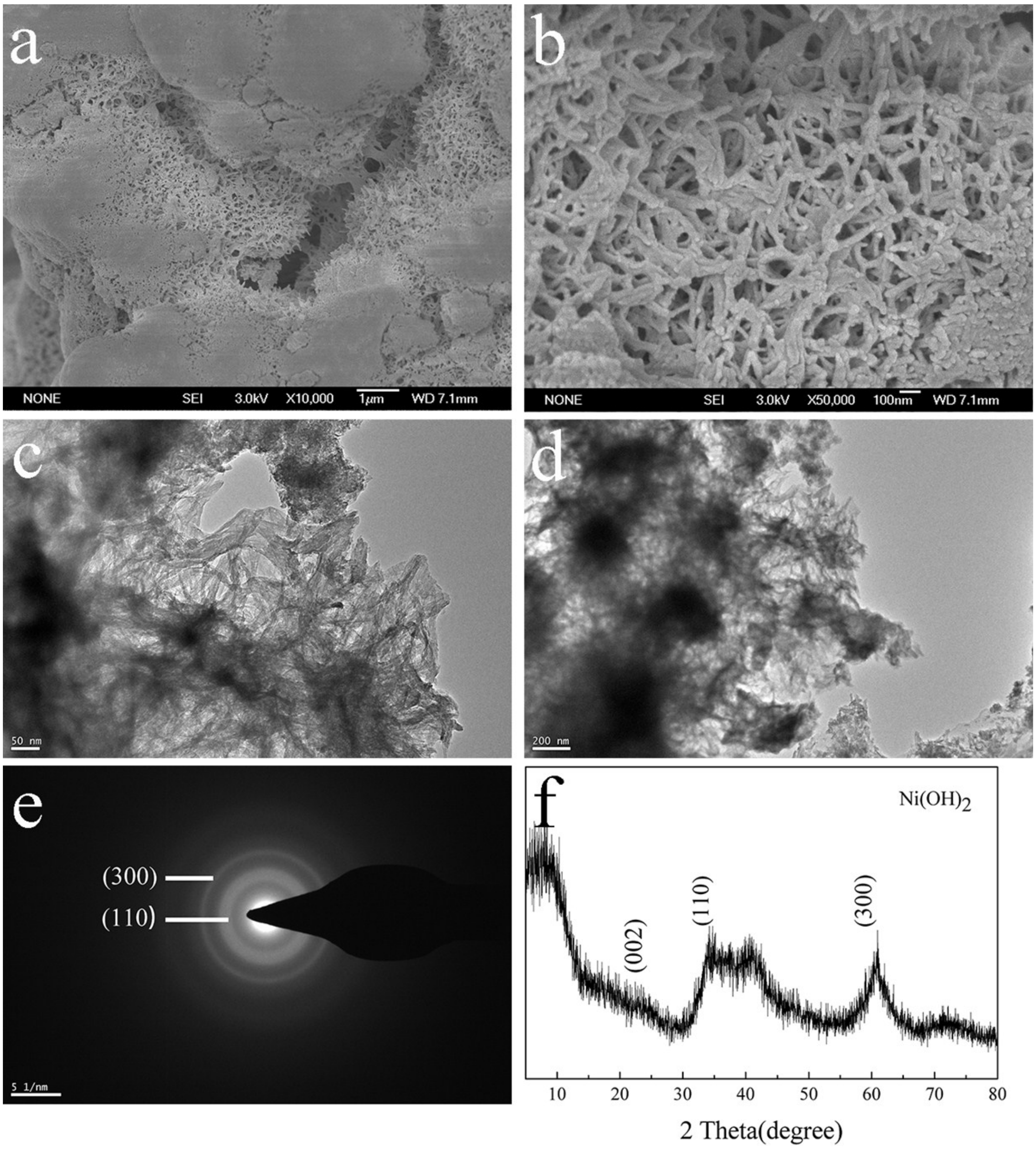

Figure S4 SEM (a and b) and TEM (c and d) images of $Ni(OH)_2$; (e) SAED pattern of $Ni(OH)_2$; and (f) XRD pattern of $Ni(OH)_2$

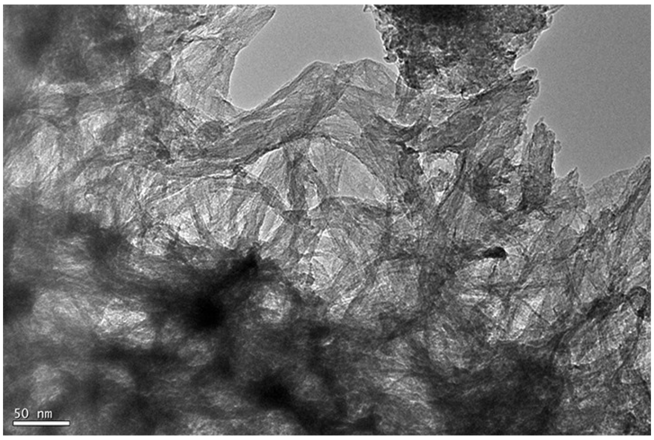

Figure S5 TEM image of $Ni(OH)_2$ in hybrid membrane

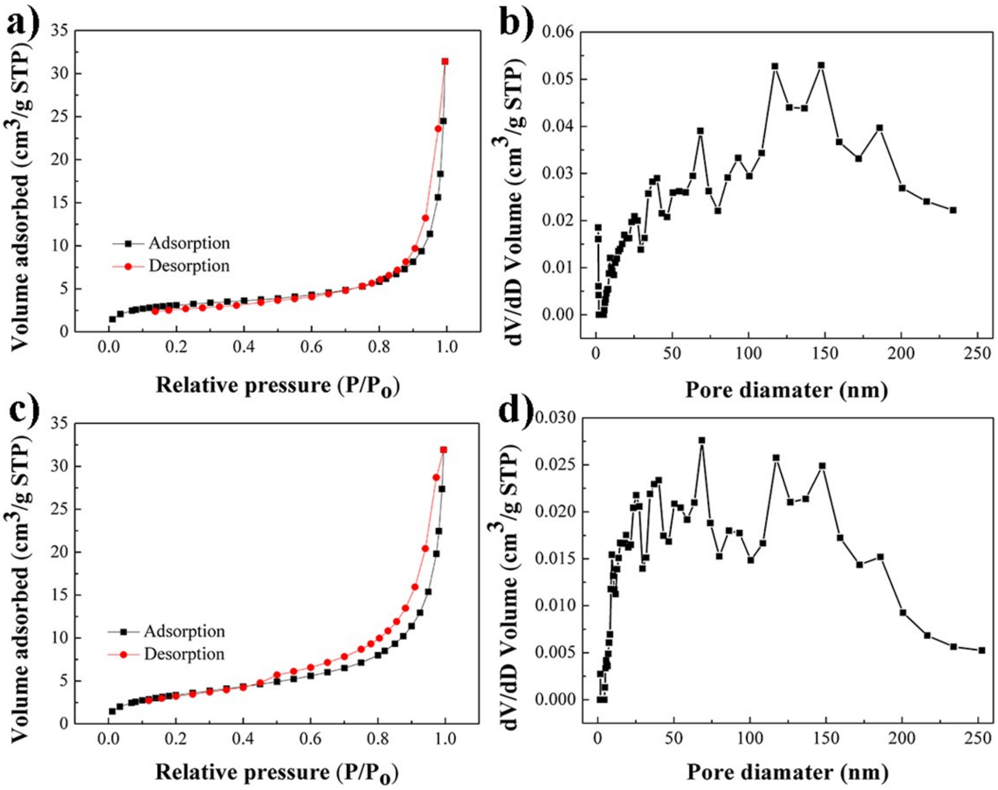

Figure S6 N_2 adsorption-desorption isotherms and pore size distributions of FME-NP (a and b) and FME-NC (c and d)

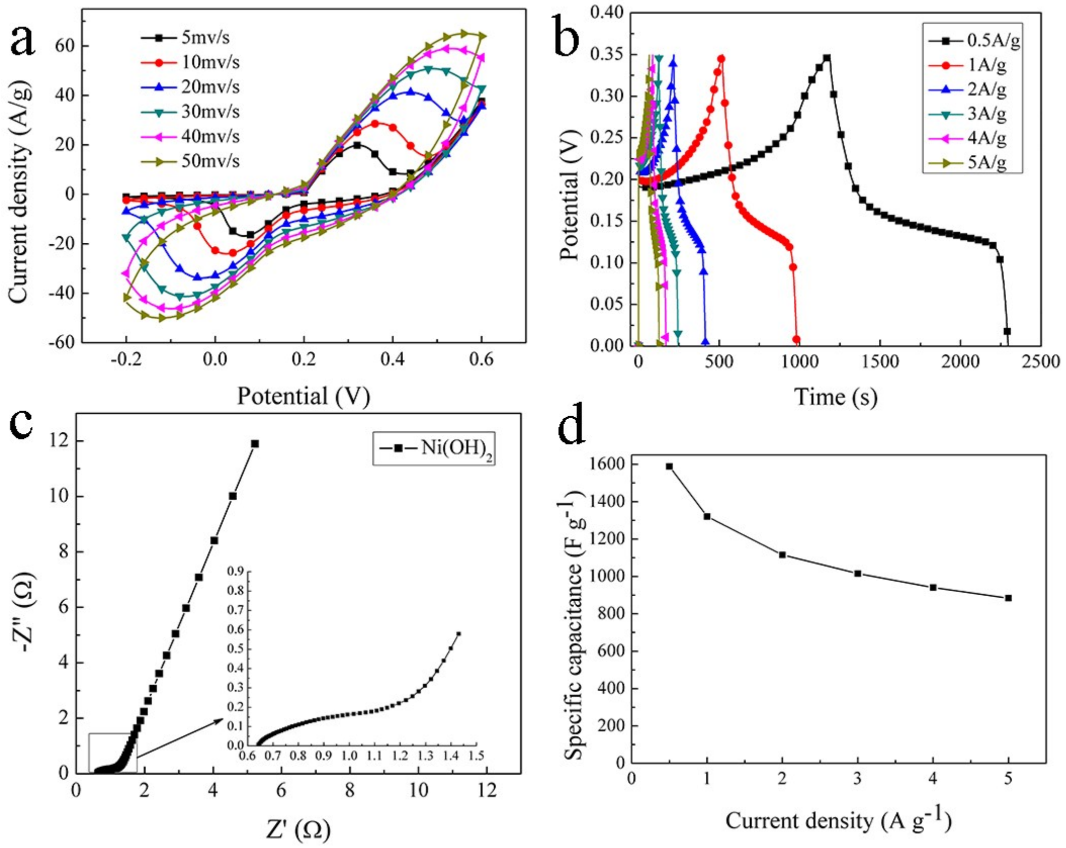

Figure S7 Electrochemical performance of pure $Ni(OH)_2$ in 6 M KOH aqueous solution: (a) CV curves at different scan rates over a potential range from -0.2 to 0.6 V; (b) GCD curves at different current densities; (c) complex-plane impedance plot; and (d) specific capacitance at different current densities

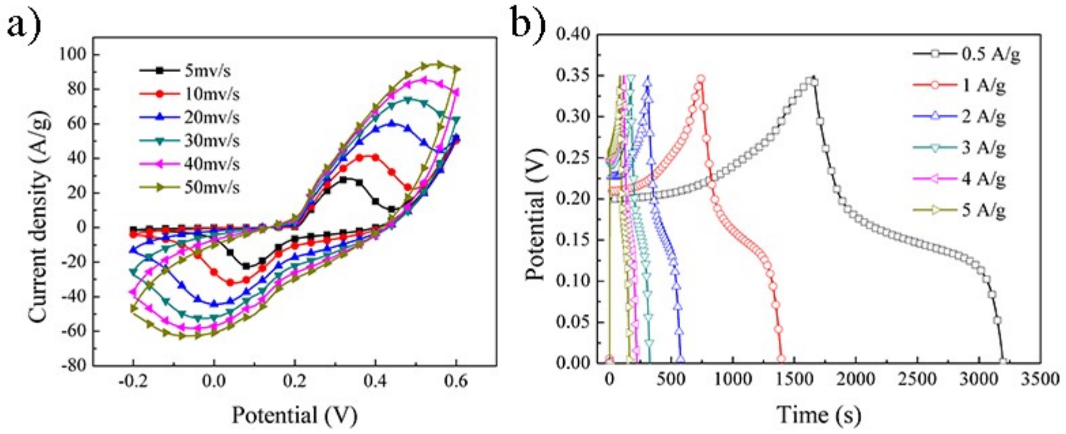

Figure S8 The electrochemical properties of FME-$Ni(OH)_2$: (a) CV curves at the different scanning rates; (b) GCD curves at various current densities

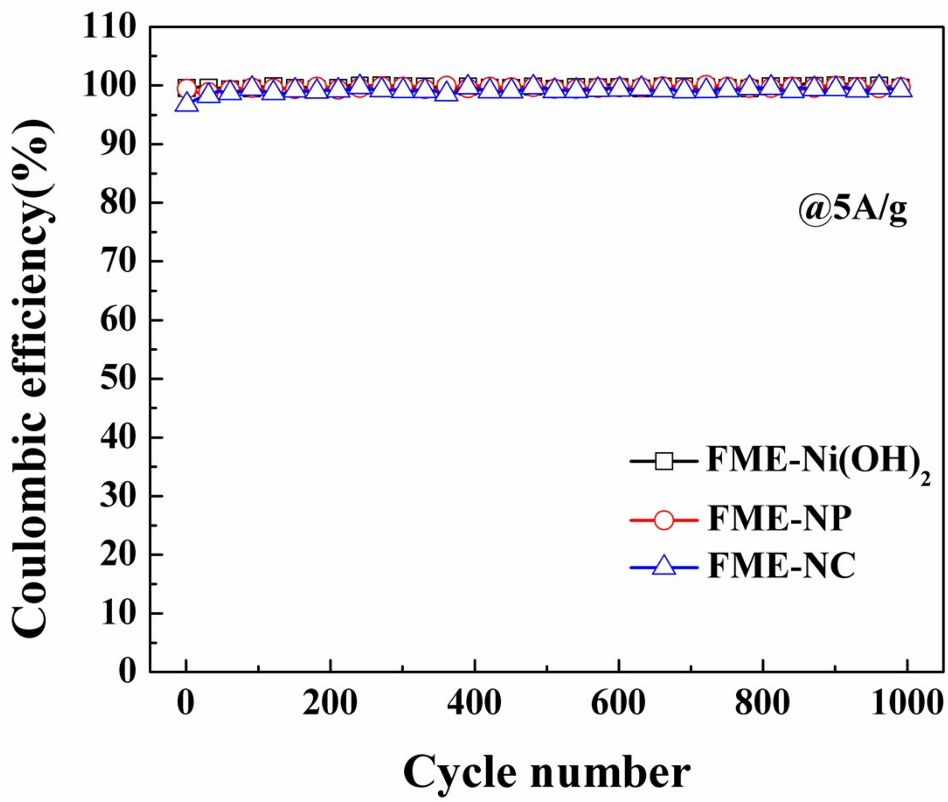

Figure S9 Coulombic efficiency of FME-Ni(OH)$_2$, FME-NP and FME-NC at a current density of 5 A/g

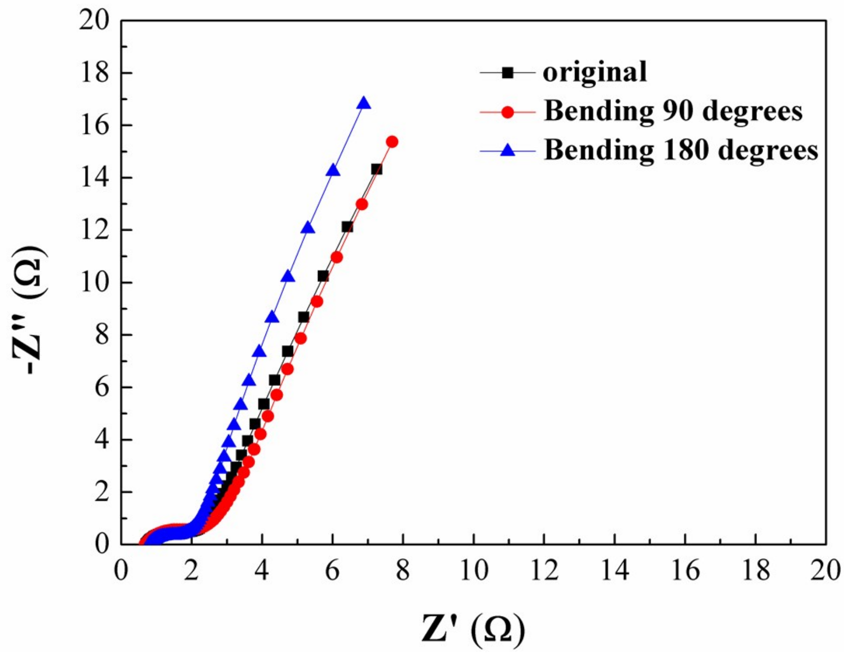

Figure S10 The electrochemical impedance spectroscopy curves of FME-Ni(OH)$_2$ at different bending states

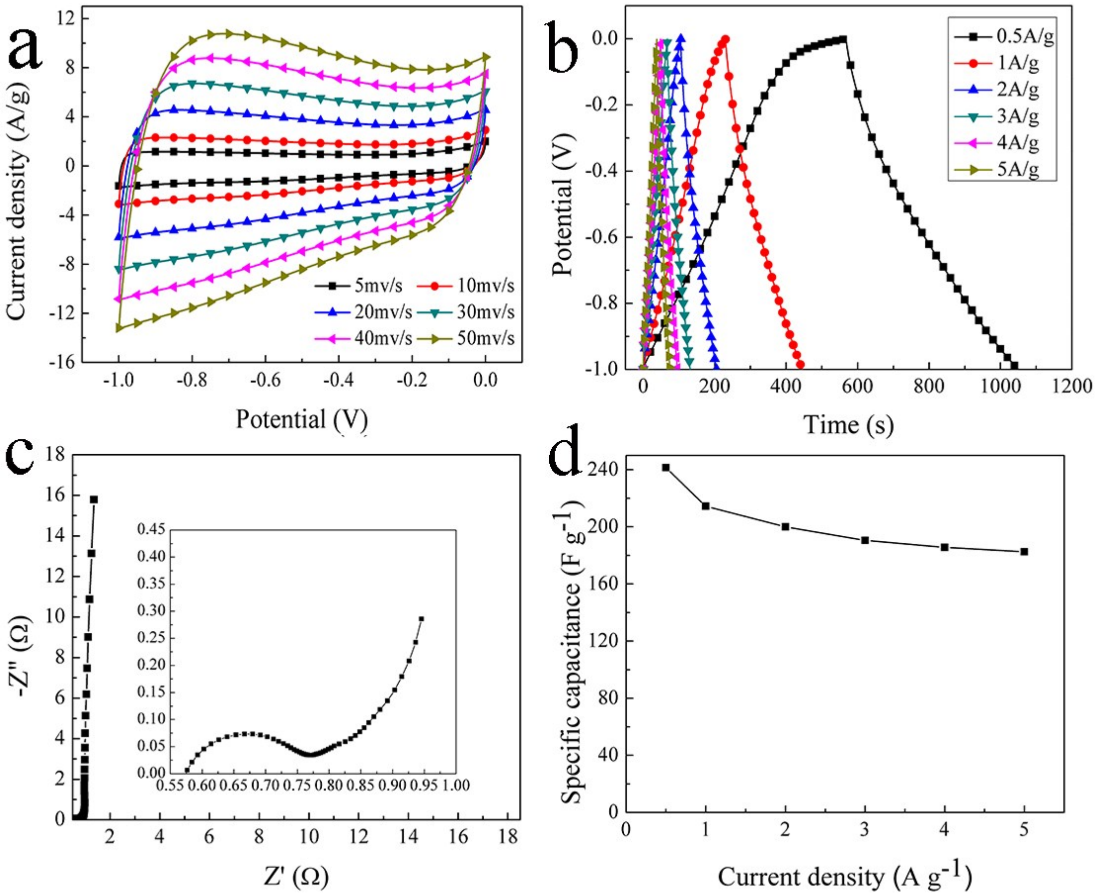

Figure S11 Electrochemical performance of FME-AC in 6 M KOH aqueous solution: (a) CV curves at different scan rates over a potential range from -1 to 0 V; (b) GCD curves at different current densities; (c) complex-plane impedance plot; and (d) specific capacitance at different current densities

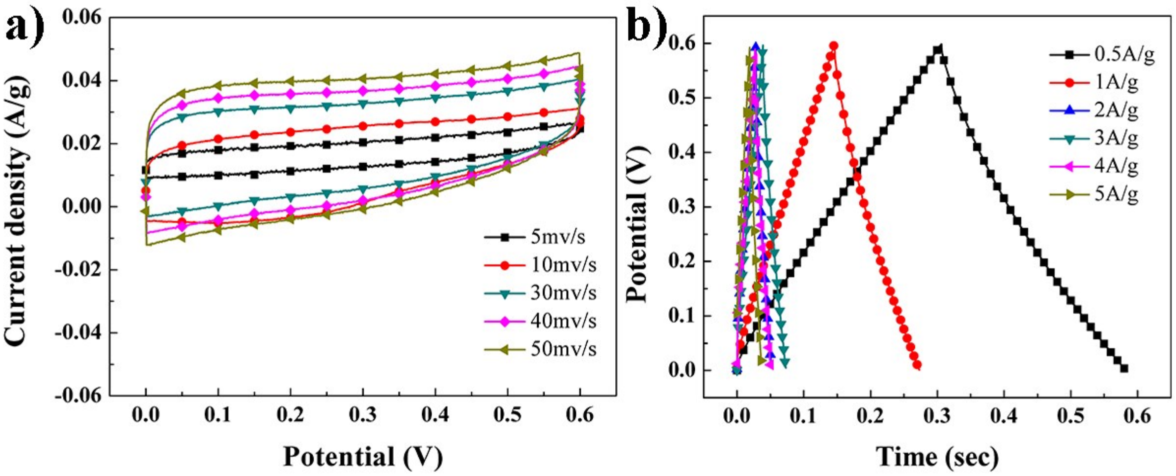

Figure S12 The electrochemical capacitance performance of FME-Ni(OH)$_2$//FME-Ni(OH)$_2$ SC device: (a) CV curves at various scanning rates; (b) GCD curves at various current densities

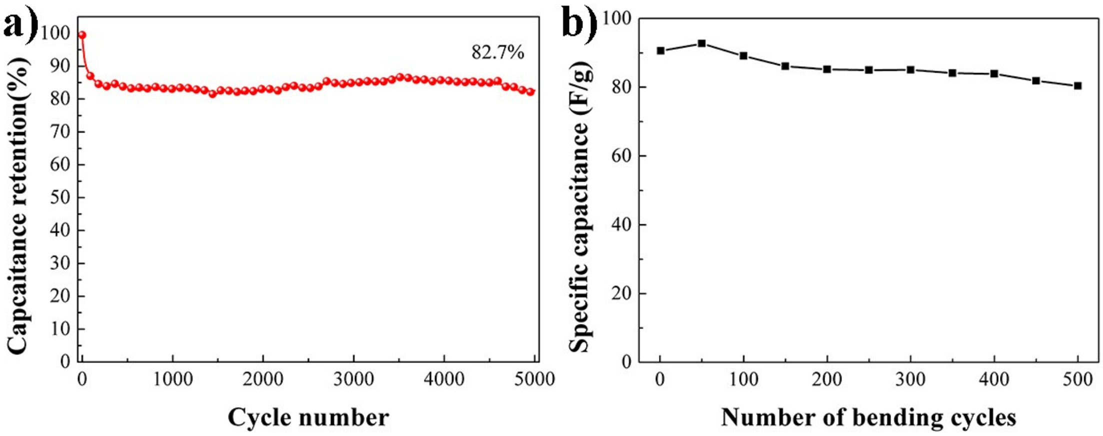

Figure S13 (a) cycle life (b) specific capacitance versus bending cycles of FME-$Ni(OH)_2$//FME-AC ASC device at a current density of 1 A/g

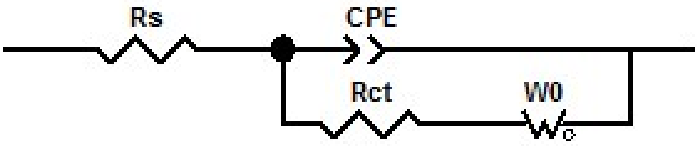

Figure S14 Equivalent circuit of all impedance spectra for different samples

Table S1 Fitted parameters for EIS obtained by Zswinpwin software of different samples

Sample	R_S (Ω)	R_{CT} (Ω)	W_0 (Ω)
FME-$Ni(OH)_2$	0.6043	0.7238	0.3129
FME-NP	0.5969	0.8969	0.3415
FME-NC	0.6491	1.811	0.2773
FME-$Ni(OH)_2$//FME-AC ASC	0.105	4.569	0.146

Table S2 The specific capacitance of different samples calculated from discharging curves

Current density			0.5	1	2	3	4	5
Specific capacitance (F/g)&(C/g)	Sample	Ni(OH)$_2$	1588.6 (556.0)	1320.6 (462.2)	1115.4 (390.4)	1015.7 (355.5)	940.8 (329.3)	884.0 (309.4)
		FME-Ni(OH)$_2$	2198.6 (769.5)	1849.1 (647.2)	1510.9 (528.8)	1318.3 (461.4)	1200.0 (420.0)	1111.9 (389.2)
		FME-NP	2210.0 (773.5)	1816.0 (635.6)	1430.3 (500.6)	1199.1 (419.7)	1049.1 (367.2)	924.0 (323.4)
		FME-NC	992.9 (347.5)	658.0 (230.3)	452.0 (158.2)	366.2 (128.2)	309.0 (108.2)	267.3 (93.6)
		FME-AC	241.4	214.4	200.0	190.5	185.6	182.5
		FME-Ni(OH)$_2$//FME-AC ASC	102.2 (163.5)	90.4 (144.6)	77.4 (123.8)	68.8 (110.1)	62.6 (100.2)	58.0 (92.8)

Table S3 The energy densities and power densities of various asymmetric supercapacitors reported in literatures

ASCs	Specific capacitance	Energy density & Power density	Current density or scan rate	Cycle life	Measurement conditions	Ref. (year)
$Ni(OH)_2$/AC/CNT//AC	82.1 F/g	32.3 Wh/kg at 504.8 W/kg	0.5 A/g	83.5 % after 1000 cycles	6 M KOH	[S4] (2015)
$Ni(OH)_2$ nano-sheets//AC	248 F/g	22 Wh/kg at 800 W/kg	1 A/g	85.7 % after 4000 cycles	6 M KOH	[S5] (2015)
$Ni(OH)_2$//AC	153 F/g	35.7 Wh/kg at 490 W/kg	5 mv/s	81 % after 10000 cycles	1 M KOH	[S6] (2013)
CNT/$Ni(OH)_2$//rGO	78 F/g	35 Wh/kg at 1800 W/kg	2 A/g	—	1 M KOH	[S7] (2015)
β-$Ni(OH)_2$/Ni-foam //AC	105.8 F/g	36.2 Wh/kg at 100.6 W/kg	0.13 A/g	92 % after 1000 cycles	6 M KOH	[S8] (2014)
Graphene@Ni$(OH)_2$ //graphene@CNT	44.8 F/g	18 Wh/kg at 850 W/kg	1 A/g	—	1 M KOH	[S9] (2014)
Graphene film //graphene film	111 F/g	15.4 Wh/kg at 554 W/kg	10 mv/s	—	2 M KCl	[S10] (2010)
rGO/CB //rGO/CB	112 F/g	9.95 Wh/kg	5 mv/s	94 % after 5000 cycles	1 M H_2SO_4	[S11] (2014)
Carbon nanofiber //carbon fiber	43.7 F/g	6.07 Wh/kg At 250 W/kg	0.5 A/g	95.9 % after 5000 cycles	2 M H_2SO_4	[S12] (2013)
FME-$Ni(OH)_2$//FME-AC	102.2 F/g	36.3 Wh/kg at 400 W/kg	0.5 A/g	88.8 % after 1000 cycles	6 M KOH	**This work**

References

[S1] T.L. John, F. Debby, S. Ronald, Functional polymers from novel carboxylterminated trithiocarbonates as highly efficient RAFT agents, Macromolecules 35 (2002) 6754–6756.

[S2] L.H. Du, P.H. Yang, X. Yu, P.Y. Liu, J.H. Song, W.J. Mai, Flexible supercapacitors based on carbon nanotube/MnO2 nanotube hybrid porous films for wearable electronic devices, Journal of Materials Chemistry A 2 (2014) 17561-17567.

[S3] H.L. Fan, F. Ran, X.X. Zhang, H.M. Song, W.X. Jing, K.W. Shen, Easy fabrication and high electrochemical capacitive performance of hierarchical porous carbon by a method combining liquid-liquid phase separation and pyrolysis process, Electrochimica Acta 138 (2014) 367–375.

[S4] L.P. Sui, S.H. Tang, Y.D. Chen, Z. Dai, H.X. Huangfu, Z.T. Zhu, X.L. Qin, Y.X. Deng, G. M. Haarberg, An asymmetric supercapacitor with good electrochemical performances based on $Ni(OH)_2$/AC/CNT and AC, Electrochimica Acta 182 (2015) 1159–1165.

[S5] W.P. Sun, X.H. Rui, M. Ulaganathan, S. Madhavi, Q.Y. Yan, Few-layered $Ni(OH)_2$ nanosheets for high-performance supercapacitors, Journal of Power Sources 295 (2015) 323–328.

[S6] H.B. Li, M.H. Yu, F.X. Wang, P. Liu, Y. Liang, J. Xiao, C.X. Wang, Y.X. Tong, G.W. Yang, Amorphous nickel hydroxide nanospheres with ultrahigh capacitance and energy density as electrochemical pseudocapacitor materials, Nature Communications 5 (2013) 54–56.

[S7] R.R. Salunkhe, J.J Lin, V. Malgras, S.X. Dou, J.H. Kim, Y. Yamauchi, Large-scale synthesis of coaxial carbon nanotube/$Ni(OH)_2$ composites for asymmetric supercapacitor application, Nano Energy 59 (2015) 211–218.

[S8] J.C. Huang, P.P. Xu, D.X. Cao, X.B. Zhou, S.N. Yang, Y.J. Li, G.L. Wang, Asymmetric supercapacitors based on beta-$Ni(OH)_2$ nanosheets and activated carbon with high energy density, Journal of Power Sources 246 (2014) 371–376.

[S9] M. Li, Z. Tang, M. Leng, J.M. Xue, Flexible solid-state supercapacitor based on graphene-based hybrid Films, Advanced Functional Materials 24 (2014) 7495–7502.

[10] A.P. Yu, I. Roes, A. Davies, Z.W. Chen, Ultrathin, transparent, and flexible graphene films for supercapacitor application, Applied Physics Letters 25 (2010)

253105.

[11] Y.M. Wang, J.C. Chen, J.Y. Cao, Y. Liu, Y. Zhou, J.H. Ouyang, D.C. Jia, Graphene/carbon black hybrid film for flexible and high rate performance supercapacitor, Journal of Power Sources 271 (2014) 269–277.

[S12] L.F. Chen, Z.H. Huang, H.W. Liang, W.T. Yao, Z.Y. Yu, S.H. Yu, Flexible all-solid-state high-power supercapacitor fabricated with nitrogen-doped carbon nanofiber electrode material derived from bacterial cellulose, Energy & Environmental Science 6 (2013) 3331–3338.